Receptor-Mediated Delivery of Magnetic Nanoparticles across the Blood–Brain Barrier

Ruirui Qiao,[†] Qiaojuan Jia,[†] Sabine Hüwel,[‡] Rui Xia,[§] Ting Liu,[§] Fabao Gao,[§,*] Hans-Joachim Galla,[‡,*] and Mingyuan Gao[†,*]

[†]Institute of Chemistry, Chinese Academy of Sciences, Bei Yi Jie 2, Zhong Guan Cun, Beijing 100190, China, [‡]Institute for Biochemistry, Westfälische Wilhelms-Universität, Wilhelm Klemm Straße 2, 48149 Münster, Germany, and [§]Molecular Imaging Laboratory, Department of Radiology, West China Hospital, Sichuan University, Chengdu 610041, China

ABSTRACT

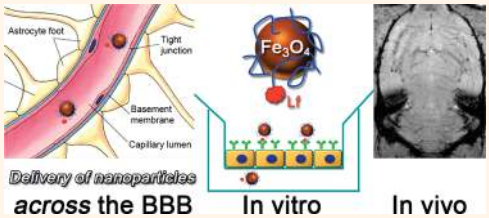

A brain delivery probe was prepared by covalently conjugating lactoferrin (Lf) to a poly(ethylene glycol) (PEG)-coated Fe_3O_4 nanoparticle in order to facilitate the transport of the nanoparticles across the blood–brain barrier (BBB) by receptor-mediated transcytosis *via* the Lf receptor present on cerebral endothelial cells. The efficacy of the Fe_3O_4-Lf conjugate to cross the BBB was evaluated *in vitro* using a cell culture model for the blood–brain barrier as well as *in vivo* in SD rats. For an *in vitro* experiment, a well-established porcine BBB model was used based on the primary culture of cerebral capillary endothelial cells grown on filter supports, thus allowing one to follow the transfer of nanoparticles from the apical (blood) to the basolateral (brain) side. For *in vivo* experiments, SD rats were used as animal model to detect the passage of the nanoparticles through the BBB by MRI techniques. The results of both *in vitro* and *in vivo* experiments revealed that the Fe_3O_4-Lf probe exhibited an enhanced ability to cross the BBB in comparison to the PEG-coated Fe_3O_4 nanoparticles and further suggested that the Lf-receptor-mediated transcytosis was an effective measure for delivering the nanoparticles across the BBB.

KEYWORDS: magnetic nanoparticle · blood–brain barrier · lactoferrin · receptor-mediated · MRI

The blood–brain barrier (BBB) is a physical and physiological barrier that regulates the passage of molecules from the systemic circulation to the brain parenchyma.[1] It is built up by the brain capillary endothelial cells connected by tight junctions and supporting pericytes and astrocytic endfeet. Only un-ionized, lipophilic, and low molecular weight molecules can diffuse freely through the endothelial membrane and may thus passively cross the BBB. Polar molecules and small ions are almost totally excluded by the tightly closed intercellular cleft.[2] While the BBB constitutes a natural defense mechanism that safeguards the brain against the invasion of various circulating toxins and infected cells, it also offers one of the most exclusive biological barriers limiting the brain uptake of diagnostic and/or therapeutic agents.[3,4]

Targeted delivery across the BBB is one of the most challenging fields of research dealing with the diagnosis and treatment of various neurological disorders.[4] In general, transport mechanisms across the BBB can be broadly divided into three types, namely, passive, carrier-mediated, and vesicular transport.[5] For example, lipid-soluble nonpolar substances can enter the brain *via* passive diffusion across the BBB. In contrast, polar substances and small peptides have to be transported across the endothelium by carrier-mediated influx. Mechanistically different is the vesicular transport facilitated by either a receptor-mediated or absorptive-mediated transcytosis, possibly induced by cationic proteins. It is broadly accepted that the use of receptor-mediated systems seems to be one of the most promising noninvasive approaches to overcome the BBB. Such an approach combines the advantages of brain targeting, high incorporation capacity, reduction of side effects, and circumvention of the multidrug efflux system.[2,6] Mammalian lactoferrin (Lf), a cationic iron-binding glycoprotein (M_w = 80 kDa) belonging to the transferrin (Tf) family, is a promising candidate for such an approach. It is involved in host defense against infection and severe inflammation and accumulates in the brain during neurodegenerative disorders.[7] The Lf receptor has been demonstrated to exist at the endothelial cells of the BBB and has been

* Address correspondence to gaomy@iccas.ac.cn; gallah@uni-muenster.de; gaofabao@yahoo.com.

Received for review January 17, 2012 and accepted March 25, 2012.

Published online March 25, 2012
10.1021/nn300240p

shown to be involved in Lf-receptor-mediated transcytosis through the BBB *in vitro* and *in vivo*.[6,8,9] Recently, it was further demonstrated that Lf is a promising brain-targeting ligand due to its higher uptake efficacy compared to transferrin and OX-26 (an anti-Tf-receptor antibody).[10] Lf was also used as a brain-targeting ligand for desgining brain drug carrier.[11,12]

Nanomaterials and nanotechnology have presented great potentials in biological analysis and clinical diagnosis.[13,14] Magnetic nanocrystals, as the core material of a new type of magnetic resonance contrast agent, have shown a bright future in early detection and treatment of diseases.[15−17] Although they are well suitable for magnetic resonance imaging (MRI), the magnetic nanoparticle-based contrast agents still suffer from the inability to cross biological barriers, such as the BBB.[18] Thus, the *in vivo* application of magnetic nanoparticles as MRI contrast agent for brain imaging is still limited and therefore challenging.

In our previous investigations, we have established different synthetic techniques for producing water-soluble,[19,20] biocompatible superparamagnetic Fe_3O_4 nanoparticles,[21] as well as biocompatible nanoparticles bearing surface reactive moieties.[22,23] Furthermore, it has been demonstrated that the resultant Fe_3O_4 nanocrystals coated by α,ω-dicarboxyl-terminated poly(ethylene glycol) (HOOC-PEG-COOH) can be used for constructing MRI and MRI-SPECT dual-modality molecular probes for *in vivo* colorectal carcinoma and gastric carcinoma detection.[22,24] The surface-coated carboxylated PEG on one hand provides biocompatibility to the nanocrystals and on the other hand offers free surface carboxyl groups for further covalently conjugating bioligands to the particles.[25,26]

Following our previous investigations, we herein report a brain delivery probe based on the PEG-coated Fe_3O_4 nanoparticles that can be used as an MRI contrast agent. PEG is known to reduce protein adsorption and limit immune recognition and thereby can effectively increase the blood circulation time of the underlying particles.[27] Moreover, PEG may increase the endothelial permeability of the nanoprobes and thus facilitate their BBB passage.[28] Therefore, PEG-coated Fe_3O_4 nanoparticles were adopted to couple with Lf for constructing a receptor-mediated transcytosis probe. The BBB transmigration efficacy of the resultant probe was evaluated using an *in vitro* BBB model based on primary porcine brain capillary endothelial cells (PBCECs) cultured on microporous filter membrane inserts within a chamber. *In vivo* animal experiments were performed to detect the passage of the nanoprobe into the brain by a 7.0 T animal MRI instrument after it was injected into the bloodstream of SD rats. In good agreement, both techniques resulted in an improved transfer efficacy for the Fe_3O_4-Lf probe in comparison to the mother particle.

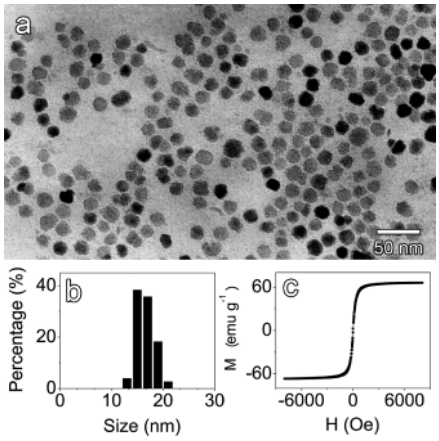

Figure 1. (a) TEM image of the PEG-coated Fe_3O_4 nanoparticles, (b) size distribution of the particles shown in frame a, (c) room-temperature magnetization curve of the PEG-coated Fe_3O_4 nanoparticles.

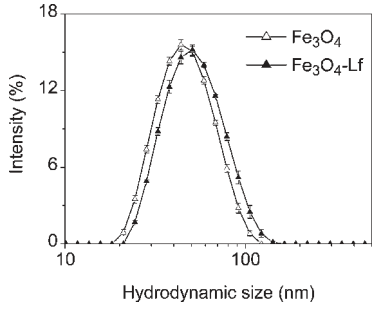

Figure 2. Hydrodynamic size distribution profiles of the PEG-coated Fe_3O_4 and the Fe_3O_4-Lf conjugate.

RESULTS AND DISCUSSION

Synthesis and Characterization of the Biocompatible Fe_3O_4 Nanoparticles. A representative transmission electron microscopy (TEM) image of the resulting biocompatible Fe_3O_4 nanoparticles is shown in Figure 1a, with the particle size distribution being depicted by a histogram shown in Figure 1b. The number-average diameter of the Fe_3O_4 nanoparticles is determined to be 16.5 ± 1.6 nm. In general, the average size of the current particle samples is much bigger than those previously synthesized and used in *in vivo* tumor detection.[24] Larger Fe_3O_4 nanoparticles were chosen instead of smaller ones on purpose due to their stronger MR contrast enhancement effect.[29] For example, the molar transversal relaxivity for 16.5 nm Fe_3O_4 particles is of 231 mM^{-1} s^{-1}, while it decreases to 92 mM^{-1} s^{-1} for 7.0 nm Fe_3O_4 particles prepared by a similar method.[25] The organic content of the current Fe_3O_4 particle sample was measured around 16.6%. As demonstrated by the room-temperature magnetization curve shown in Figure 1c, the PEG-coated Fe_3O_4 nanocrystals are superparamagnetic and present a saturation magnetization of 66.0 emu/g, corresponding to 79.1 emu per gram of Fe_3O_4, higher than their smaller counterparts published previously.[22,24] Moreover, the PEG coating

endows the Fe_3O_4 nanoparticles with excellent colloidal stability in both physiological saline and fetal bovine serum,[24] which makes them very suitable for *in vivo* bioapplications.

Conjugation of Lactoferrin to Fe_3O_4 Nanoparticles. The Fe_3O_4-Lf conjugate was prepared by the classical (EDC/sulfo-NHS)-mediated amidation reaction. The covalent coupling between Fe_3O_4 and Lf was first investigated by the dynamic light scattering (DLS) method. The results shown in Figure 2 reveal that the initial hydrodynamic size of the Fe_3O_4 nanoparticles is 43.6 nm, while the hydrodynamic size of the conjugates increases to 48.9 nm. The reasonable increase in the hydrodynamic size strongly suggests that Lf was effectively coupled to the PEG-coated Fe_3O_4 nanoparticles *via* the (EDC/sulfo-NHS)-mediated amidation reaction. Moreover, the size distribution profile of the resultant conjugates, characterized by the polydispersity index, *i.e.*, 0.348, remains nearly unchanged in comparison with that of the mother particles, *i.e.*, 0.386, which suggests that no particle coagulation occurred during the coupling reaction. To further quantify the composition of the resultant probe, the Bradford method was adopted to determine the protein content in the purified Fe_3O_4-Lf probe. According to protein assay results, approximately 14.4 Lf molecules were bound to each Fe_3O_4 nanoparticle on average.

Transendothelial Electrical Resistance (TEER) Experiment. A high yield of about 50 million endothelial cells per porcine brain and some similarities between porcine and human vascular physiology make the porcine model suitable for high-throughput drug screening.[30,31] The tight paracellular barrier is a fundamental characteristic of the BBB. Until now, TEER has been demonstrated to be one of the most straightforward methods to reveal the integrity of the BBB model and to determine the barrier properties. Moreover the impedance measurement is a reliable technique to allow a perfect online control.[32,33] Commonly, TEER is expressed as measured resistance multiplied by the area of the endothelial monolayer, which is given by the filter size, and thus the unit is Ω cm^2. Tight junctions between bordering endothelial cells are responsible for a very high transendothelial electrical resistance, which in our model approaches 1500−2000 Ω cm^2.[34−36] It has been shown that the TEER in this model directly correlates to the permeability for paracellular markers such as sucrose.[31]

In general, the TEER can be used to reveal the integrity of the *in vitro* BBB model; therefore TEER measurements were carried out before and during the incubation with the Fe_3O_4-Lf or the PEG-coated Fe_3O_4 to continuously monitor the integrity of the BBB. It is worth mentioning the fact that there are several reports published about the *in vitro* BBB model incubated with nanoparticles but without proving the BBB integrity, *e.g.*, by TEER experiment.[37] However, from our point of view, without information about the barrier integrity it is difficult to draw conclusions on the passage of particles through the BBB, irrespective of the low cell toxicity of some particle samples. Therefore, the *in vitro* BBB model used herein was carefully chosen according to its TEER value, which was typically above 700 Ω cm^2 after 7 days in culture. Then, the Fe_3O_4-Lf conjugate and the PEG-coated Fe_3O_4 nanoparticle were applied to further investigate their permeation.

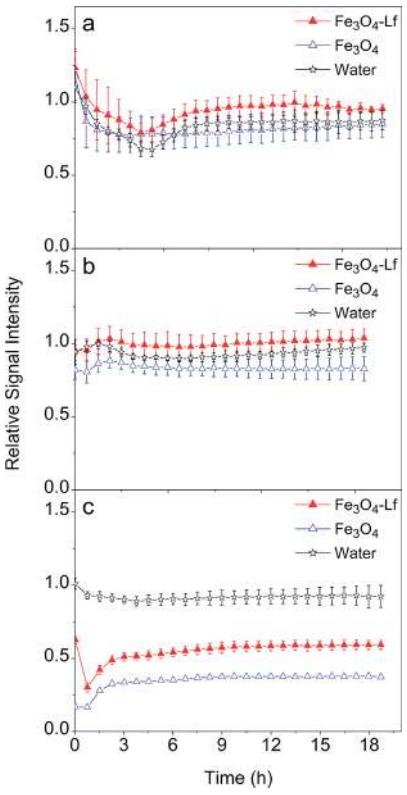

Figure 3. Normalized TEER values of PBCECs recorded after the introduction of particles with concentrations of 0.04 mg Fe/mL (a); 0.1 mg Fe/mL (b); 0.3 mg Fe/mL (c), and water as reference, respectively.

As stated in the Experimental Section, three concentrations of the Fe_3O_4-Lf and Fe_3O_4 were used in the TEER measurements, *i.e.*, 0.04 mg Fe/mL, 0.1 mg Fe/mL, and 0.3 mg Fe/mL with an identical volume of water as reference for the particle samples. All the impedance data determined were further normalized according to the initial values measured before the addition of either Fe_3O_4-Lf, Fe_3O_4, or water. The results are shown in Figure 3.

At concentration of 0.04 mg Fe/mL, the TEER values of both Fe_3O_4-Lf and Fe_3O_4 systems decrease within the initial few hours of incubation and then recover with time during prolonged incubation. Since a similar signal drop is also present in the reference sample (water), it can be concluded that the initial signal drops result from the fluctuation of the cellular systems caused by the introduction of additional sample solutions, which has been reported before.[38] Taking the

TABLE 1. Fe Concentration of the Basolateral Medium Obtained after 18 h Incubation of the Fe_3O_4-Lf or PEG-Coated Fe_3O_4 Particles in the Medium of the Apical Side

	initial Fe conc at the apical side (mg/mL)	final Fe conc at the basolateral side (mg/mL)	transport efficacy[a] (%)
Fe_3O_4	0.04	0.0045 ± 0.0003	22.5 ± 1.4
Fe_3O_4-Lf		0.0094 ± 0.0028	47.0 ± 13.8
Fe_3O_4	0.1	0.0048 ± 0.0006	9.6 ± 1.3
Fe_3O_4-Lf		0.0110 ± 0.0015	22.0 ± 2.9

[a] The transport efficacy was calculated by dividing the feeding amount of Fe by the product of the Fe concentration of the basolateral medium and its volume, which is 1 mL.

signal variation in the reference sample (water) into consideration, Fe_3O_4-Lf leads to increased TEER signals in comparison with the control particle at a concentration of 0.04 mg Fe/mL. This tendency is further enhanced and better seen when the particle concentration is increased to 0.1 mg Fe/mL (Figure 3b). Meanwhile, the TEER signal of the Fe_3O_4 system becomes lower than that of the reference. In contrast, Fe_3O_4-Lf still presents higher signals than the reference. Therefore, it can be concluded that the integrity of the *in vitro* BBB model remains rather intact in the presence of the Fe_3O_4-Lf conjugate at concentrations of both 0.04 and 0.1 mg Fe/mL. However, when the particle concentration is further increased to 0.3 mg Fe/mL, the overall TEER values of the Fe_3O_4-Lf conjugate and the control nanoparticle (the PEG-coated Fe_3O_4) are much lower than those recorded from the reference, although the early stage of decrease-and-recovery remains, which suggests that both the Fe_3O_4-Lf conjugate and the mother Fe_3O_4 particle can cause considerable damage to tight junctions of the *in vitro* BBB model but only at high concentration. Nevertheless, the Fe_3O_4-Lf conjugate exhibits higher TEER values than the mother Fe_3O_4 nanoparticle at all three concentrations, suggesting that the covalently conjugated Lf is able to protect the tight junctions of the *in vitro* BBB model from being damaged by the Fe_3O_4 nanoparticles. Further experiments by incubating Lf with the PBCECs confirmed that Lf itself can increase the TEER value (Figure S1 in the Supporting Information (SI)) owing to the Lf-receptor interaction on the PBCECs. It is worth mentioning that the cell layer's capacitance results, as shown in Figure S2 in the SI, suggest that the PBCECs can survive the whole incubation process even when the particle concentration reaches 0.3 mg/mL.

Determination of the Permeation of the Fe_3O_4-Lf Conjugate across the BBB *in Vitro*. The medium at the basolateral side was collected after approximately 18 h of incubation in the presence of either Fe_3O_4-Lf or Fe_3O_4 particles. To evaluate the efficacy of the particle transport across the BBB, the iron content in the medium of the basolateral side was analyzed by the AAS method. The results shown in Table 1 reveal that the transport

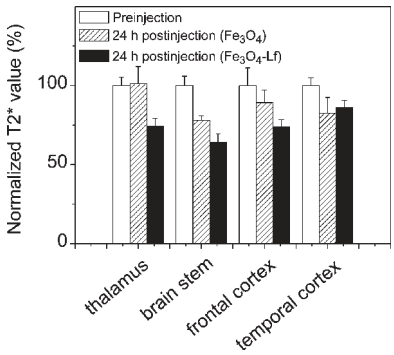

Figure 4. Relative T2* value of different brain regions extracted from T2* MR images of SD brains before and after the injection of Fe_3O_4-Lf or Fe_3O_4.

efficacy achieved at Fe_3O_4 particle concentrations of 0.04 mg and 0.1 mg Fe/mL is strongly enhanced after Lf was conjugated to Fe_3O_4. In general, nanoobjects cannot pass through the BBB.[18,39] However, quite unexpectedly, the current results suggest that Fe_3O_4 nanoparticles coated by PEG also have a certain ability to pass through the BBB model, which can reasonably be attributed to the PEG coating due to its amphiphilic nature.[18] A temporary barrier-opening effect of detergent-coated poly-*n*-butylcyano-acrylate nanoparticles accompanied by an enhanced nanoparticle transport across the BBB was also reported recently.[40] Therefore, it is necessary to verify the Lf-mediated mechanism for the transport of the Fe_3O_4-Lf probe across the BBB. A further blocking study demonstrated that the transport efficacy dropped from 22.0 ± 2.9% to 1.0 ± 0.6%, in the presence of 16 times the lactoferrin in the apical medium, for the Fe_3O_4-Lf probe at a concentration of 0.1 mg Fe/mL. Therefore, the remarkably increased transport efficacy for the Fe_3O_4-Lf probe in contrast to the mother particles can be attributed to the receptor-mediated transcytosis, which facilitates the Fe_3O_4 particle crossing of the BBB.

Fe_3O_4-Lf across the BBB *in Vivo*. Following the successful *in vitro* experiments, animal experiments were carried out for further investigating the Lf-mediated transport of the Fe_3O_4 nanoparticles across the BBB *in vivo* using SD rats as an animal model. In detail, both coronal and axial T2*-weighted MR images of pre- and 24 h postinjection of the probes were acquired. The normalized T2* values of thalamus, brain stem, frontal cortex, and temporal cortex were extracted and are shown in Figure 4. Except for the temporal cortex region, the Fe_3O_4-Lf conjugates show stronger effects in reducing the T2* value in comparison with the mother Fe_3O_4 nanoparticles, which further supports the Lf-receptor-mediated transport of the Fe_3O_4 particles across the BBB *in vivo*. In comparison with the precontrast group, the Fe_3O_4 group also showed some decreases in T2* values at the location of brain stem, frontal cortex, and temporal cortex, which is also consistent with the *in vitro* experimental results.

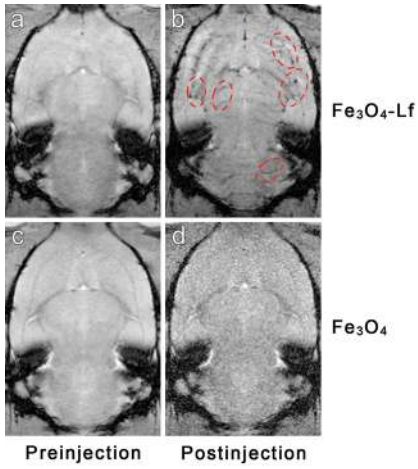

Figure 5. Axial T2* images of rat brains captured preinjection and 15 min postinjection of Fe_3O_4-Lf and Fe_3O_4, respectively. The red dashed-line circles highlight the brain blood vessels enhanced by the Fe_3O_4-Lf probe.

Representative T2* images acquired before and 15 min after the injection of the Fe_3O_4-Lf conjugate or PEG-coated Fe_3O_4 nanoparticles are shown in Figure 5. The Fe_3O_4-Lf probe exhibits a stronger contrast-enhanced vascular imaging effect than the mother Fe_3O_4 nanoparticle. Although both the Fe_3O_4-Lf probe and the mother Fe_3O_4 nanoparticle can give rise to decreased T2* values at 24 h postinjection, as shown in Figure 4, the vascular specificity of the Fe_3O_4-Lf probe shown at the early stage of postinjection strongly indicates that the Fe_3O_4-Lf conjugate interacts with the Lf receptor on the surface of the brain microvascular tissue through the specific interactions between Lf and its receptor. Moreover, the greatly reduced vascular specificity against time, as shown in Figure S3, implies that the Fe_3O_4-Lf conjugates were not stuck in the endothelial cells during the transcytosis. Over the long run, the mother Fe_3O_4 particle also presents a certain degree of enhancement effect for the brain. Since no brain vascular specificity was observed from the mother particle, it can be deduced that the PEG-coated Fe_3O_4 nanoparticles cross the BBB *via* a different mechanism but with a low efficacy.[24]

CONCLUSION

In summary, we have successfully developed a brain delivery probe by covalently conjugating lactoferrin to the PEG-coated Fe_3O_4 nanoparticles to achieve receptor-mediated delivery of nanoparticles across the BBB. The *in vitro* BBB model experimental results suggest that the PEG coating favors the transfer of the underlying particles across the intact BBB model, while this effect is effectively enhanced by the covalently attached lactoferrin. In good agreement with the *in vitro* experimental results, further *in vivo* animal experiments show a similar tendency but also show a clear vascular imaging ability of the Fe_3O_4-Lf probe during the early stage of postinjection, which strongly supports that brain delivery is achieved *via* the lactoferrin-receptor-mediated pathway. The current investigations further suggest that the PEG-coated nanoparticles, apart from acting as brain MRI contrast agent, can potentially be used as a brain delivery vehicle for molecules of interest for brain diseases by further coupling the magnetic particles with diagnostic, therapeutic, and/or curative effect tracking reagents using the particle surface carboxyl groups.

EXPERIMENTAL SECTION

Chemicals. Iron(III) acetylacetonate ($Fe(acac)_3$) was purchased from Aldrich (14024-18-1) and used after two recrystallizations. Analytical grade chemicals such as ethanol, ether, and diphenyl oxide were purchased from Sinopharm Chemical Reagent Beijing, Co., Ltd. Diphenyl oxide was used after further purification by reduced pressure distillation. EDC (1-ethyl-3-(3-dimethylaminopropyl carbodiimide), 39391) and sulfo-NHS (*N*-hydroxysulfosuccinimide sodium salt, 56485) were purchased from Fluka. HOOC-PEG-COOH was synthesized according to ref 21. Lactoferrin was purchased from Sigma-Aldrich (L9507). Bradford reagent for protein analysis was purchased from Sigma-Aldrich (B6916). For constructing the BBB *in vitro* model, collagen G, medium 199, Dulbecco's modified Eagle's medium/Ham's F12, new born calf serum, L-glutamine, gentamycin, penicillin, and streptomycin were all purchased from Biochrom, Berlin, Germany. Puromycin and hydrocortisone were purchased from Sigma-Aldrich.

Preparation of Biocompatible Fe_3O_4 Nanoparticles. The biocompatible Fe_3O_4 nanoparticles were synthesized by a modified "one-pot" synthetic approach according to our previous reports.[24,25] Typically, 2.1 g of $Fe(acac)_3$ (6 mmol), 7.9 mL of oleylamine (24 mmol), and 24 g of HOOC-PEG-COOH (12 mmol, $M_n = 2000$) were dissolved in 100 mL of diphenyl ether solution. The solution was purged with nitrogen for 2 h to remove oxygen under mechanical stirring at 400 rpm. After being incubated at 80 °C for 4 h, the reaction mixture was quickly heated to reflux within 10 min and maintained at reflux for 30 min. Ether was used to precipitate the resultant Fe_3O_4 nanocrystals out of the reaction mixture after it was cooled to room temperature. Then, the precipitate was redissolved in ethanol followed by addition of ether as precipitant. Typically, this purifying procedure was repeated for three cycles. The PEG-coated Fe_3O_4 nanocrystals finally obtained were dissolved in either Milli-Q water or PBS (phosphate-buffered saline) for further experiments.

Characterization of Fe_3O_4 Nanoparticles. TEM images were obtained using a transmission electron microscope (JEM-100CXII) operating at an accelerating voltage of 100 kV. The average equivalent area diameter of the Fe_3O_4 nanoparticles was obtained by measuring more than 400 quasi-spherical particles. Magnetization measurements were performed by using a vibrating sample magnetometer (VSM JDM-13, China). The hydrodynamic size of the samples was characterized at 298.0 K by a DLS using an instrument (Nano ZS, Malvern) equipped with a solid-state He−Ne laser (λ = 633 nm). The organic content was measured by thermogravimetry analysis (TG/DTA 6300, SII Nanotechnology Inc.).

Preparation of Fe_3O_4-Lf Covalent Conjugate. Typically, EDC (2.50 μmol) and sulfo-NHS (6.25 μmol) were dissolved in 950 μL of a 0.01 M PBS buffer solution containing 2.0 mg of Fe_3O_4 nanocrystals. After approximately 15 min, 50 μL of a 0.01 M PBS buffer solution containing 0.5 mg of Lf was introduced. The reaction was run overnight at 4 °C. The resultant conjugates were collected at 13 000 rpm/min to remove the impurities and

unreacted Lf molecules and then redissolved in PBS (1 mL) and kept at 4 °C until further use. The coupling reaction between Fe_3O_4 particles and Lf was investigated *via* the DLS method by monitoring the variation in the hydrodynamic size of the nanoparticles before and after the conjugation reaction. The amount of Lf in the resultant conjugate was quantified by the Bradford method. The reaction time of the Bradford procedure was set to 5 min. Quite probably due to the interference of Fe_3O_4, a prolonged incubation time was found to lead to an overestimated protein content.

Preparation and Cultivation of PBCECs. The primary culture of PBCECs was performed by a modified method described by Franke *et al.*[36] Briefly, PBCECs were isolated from the brains of freshly slaughtered six-month-old pigs. After isolation, cells were seeded in culture flasks (Nunc, Wiesbaden, Germany) coated with collagen G and cultured in plating medium (Medium 199 supplemented with 10% newborn calf serum, 0.7 mM L-glutamine, 100 μg/mL gentamycin, 100 U/mL penicillin, 100 μg/mL streptomycin) at 37 °C in humidified air with 5% CO_2. Possible contaminating pericytes within the endothelial cultures were removed according to Perriere *et al.* by adding 2 μg/mL puromycin to the medium.[41] PBCECs were trypsinized at 20 °C on day 2 *in vitro* (DIV 2), frozen, and then stored in liquid nitrogen.

***In Vitro* BBB Model Studies.** For the construction of the BBB *in vitro* model, the PBCECs were gently thawed, suspended in plating medium, and seeded on rat tail collagen-coated polycarbonate membranes (Transwell, No. 3401 Costar; Corning, Wiesbaden, Germany; 0.4 μm pore size; 1.13 cm^2 growth area) with a density of 250 000 cells/cm^2. After the cells reached confluence (in general after 48 h, DIV 5), plating medium was replaced by chemically defined medium (Dulbecco's modified Eagle's medium/Ham's F12 containing 4.1 mM L-glutamine, 100 μg/mL streptomycin, and 550 nM hydrocortisone). On DIV 7, the TEER value of the PBCECs was measured, and the cells with TEER values above 700 Ω cm^2 were selected for the transfer experiments. The Fe_3O_4-Lf probe, with concentrations of 0.04, 0.1, and 0.3 mg/mL, was introduced into the apical side chamber (blood side *in vivo*) of the BBB model. The TEER values were measured during the incubation. After 18 h of incubation, the basolateral medium was collected for analyzing the iron content. In parallel, the same procedures were also applied for the control experiments based on the Fe_3O_4 nanoparticle with the same concentrations.

To provide further evidence for the Lf-mediated transcytosis mechanism, a blocking study was carried out by incubating 0.1 mg/mL Fe_3O_4-Lf probe in the apical side in the presence of 16 times the lactoferrin. Then, the iron content of the basolateral medium, collected after 18 h of incubation, was determined for further comparing with the results obtained in the absence of excessive lactoferrin.

TEER Measurements. The TEER measurements were performed by using a device reading 24 electrodes in parallel (Cellzscope, NanoAnalytics, Münster, Germany), which allows automated and continuous long-term monitoring measurements.

Determination of Fe_3O_4 Nanoparticles across the BBB *in Vitro*. Graphite furnace atomic absorption spectrometry (the Perkin-Elmer AAS) was adopted to determine the iron content of the culture medium of the basolateral side.

Animal Model and *in Vivo* MRI Experiments. MR imaging of rats with two in each group was performed before and after the injection of PEG-coated Fe_3O_4 nanoparticles or the Fe_3O_4-Lf -conjugate (10 mg Fe/(kg body weight)) by using a 7.0 T Bruker Biospec 70/30 USR nuclear magnetic resonance spectrometer. Groups of male SD rats with an average weight of 250 g were selected. The initial concentration of the Fe_3O_4 and Fe_3O_4-Lf was 2 mg/mL. After anesthetizing the rats with a gas mixture of oxygen and isoflurane, the coronal and axial images were recorded by using a Bruker BGA-S coil. MR images were acquired before and 10 min, 4 h, and 24 h after the intravenous injection of the particle probes. A T2* mapping sequence was used, and the parameters were set as follows: field of view = 3.2 × 3.2 cm^2; matrix size = 256 × 256; slice thickness = 1 mm; echo time = 4, 11, 18, 25, 32, 39, 46, 53, 60, 67, 74, 81 ms; repetition time = 1500 ms; number of excitations = 1.

Conflict of Interest: The authors declare no competing financial interest.

Acknowledgment. The current investigations are jointly supported by a NSFC Major International Joint Research Project (20820102035), a National Basic Research Program of China (973 Program, 2011CB935800), and three other NSFC projects (21003135, 81090271, 21021003). R.Q. is grateful to Prof. Helmuth Möhwald from MPIKG for kind support and stimulating discussion.

Supporting Information Available: This material is available free of charge via the Internet at http://pubs.acs.org.

REFERENCES AND NOTES

1. Ballabh, P.; Braun, A.; Nedergaard, M. The Blood-Brain Barrier: an Overview—Structure, Regulation, and Clinical Implications. *Neurobiol. Dis.* **2004**, *16*, 1–13.
2. Calvo, P.; Gouritin, B.; Chacun, H.; Desmaele, D.; D'Angelo, J.; Noel, J. P.; Georgin, D.; Fattal, E.; Andreux, J. P.; Couvreur, P. Long-Circulating PEGylated Polycyanoacrylate Nanoparticles as New Drug Carrier for Brain Delivery. *Pharm. Res.* **2001**, *18*, 1157–1166.
3. Begley, D. J. Delivery of Therapeutic Agents to the Central Nervous System: the Problems and the Possibilities. *Pharmacol. Ther.* **2004**, *104*, 29–45.
4. Orive, G.; Ali, O. A.; Anitua, E.; Pedraz, J. L.; Emerich, D. F. Biomaterial-Based Technologies for Brain anti-Cancer Therapeutics and Imaging. *Biochim. Biophys. Acta-Rev. Cancer* **2010**, *1806*, 96–107.
5. Abbott, N. J.; Ronnback, L.; Hansson, E. Astrocyte-Endothelial Interactions at the Blood-Brain Barrier. *Nat. Rev. Neurosci.* **2006**, *7*, 41–53.
6. Hu, K. L.; Li, J. W.; Shen, Y. H.; Lu, W.; Gao, X. L.; Zhang, Q. Z.; Jiang, X. G. Lactoferrin-Conjugated PEG-PLA Nanoparticles with Improved Brain Delivery: *In Vitro* and *in Vivo* Evaluations. *J. Controlled Release* **2009**, *134*, 55–61.
7. Gonzalez-Chavez, S. A.; Arevalo-Gallegos, S.; Rascon-Cruz, Q. Lactoferrin: Structure, Function and Applications. *Int. J. Antimicrob. Agents* **2009**, *33*, 301.e1–301.e8.
8. Fillebeen, C.; Descamps, L.; Dehouck, M. P.; Fenart, L.; Benaissa, M.; Spik, G.; Cecchelli, R.; Pierce, A. Receptor-Mediated Transcytosis of Lactoferrin through the Blood-Brain Barrier. *J. Biol. Chem.* **1999**, *274*, 7011–7017.
9. Huang, R. Q.; Ke, W. L.; Qu, Y. H.; Zhu, J. H.; Pei, Y. Y.; Jiang, C. Characterization of Lactoferrin Receptor in Brain Endothelial Capillary Cells and Mouse Brain. *J. Biomed. Sci.* **2007**, *14*, 121–128.
10. Ji, B.; Maeda, A.; Higuchi, M.; Inoue, K.; Akita, H.; Harashima, H.; Suhara, T. Pharmacokinetics and Brain Uptake of Lactoferrin in Rats. *Life Sci.* **2006**, *78*, 851–855.
11. Yu, Y.; Pang, Z. Q.; Lu, W.; Yin, Q.; Gao, H. L.; Jiang, X. G. Self-Assembled Polymersomes Conjugated with Lactoferrin as Novel Drug Carrier for Brain Delivery. *Pharm. Res.* **2012**, *29*, 83–96.
12. Huang, R. Q.; Ke, W. L.; Han, L.; Liu, Y.; Shao, K.; Jiang, C.; Pei, Y. Y. Lactoferrin-Modified Nanoparticles Could Mediate Efficient Gene Delivery to the Brain *in Vivo*. *Brain Res. Bull.* **2010**, *81*, 600–604.
13. Farokhzad, O. C.; Langer, R. Nanomedicine: Developing Smarter Therapeutic and Diagnostic Modalities. *Adv. Drug Delivery Rev.* **2006**, *58*, 1456–1459.
14. Veiseh, O.; Gunn, J. W.; Zhang, M. Design and Fabrication of Magnetic Nanoparticles for Targeted Drug Delivery and Imaging. *Adv. Drug Delivery Rev.* **2010**, *62*, 284–304.
15. Qiao, R. R.; Yang, C. H.; Gao, M. Y. Superparamagnetic Iron Oxide Nanoparticles: from Preparations to *in Vivo* MRI Applications. *J. Mater. Chem.* **2009**, *19*, 6274–6293.
16. Cheon, J.; Lee, J.-H. Synergistically Integrated Nanoparticles as Multimodal Probes for Nanobiotechnology. *Acc. Chem. Res.* **2008**, *41*, 1630–1640.
17. Sun, C.; Lee, J. S. H.; Zhang, M. Q. Magnetic Nanoparticles in MR Imaging and Drug Delivery. *Adv. Drug Delivery Rev.* **2008**, *60*, 1252–1265.
18. Veiseh, O.; Sun, C.; Fang, C.; Bhattarai, N.; Gunn, J.; Kievit, F.; Du, K.; Pullar, B.; Lee, D.; Ellenbogen, R. G.; *et al.* Specific Targeting of Brain Tumors with an Optical/Magnetic

Resonance Imaging Nanoprobe across the Blood-Brain Barrier. *Cancer Res.* **2009**, *69*, 6200–6207.
19. Li, Z.; Sun, Q.; Gao, M. Y. Preparation of Water-Soluble Magnetite Nanocrystals from Hydrated Ferric Salts in 2-Pyrrolidone: Mechanism Leading to Fe_3O_4. *Angew. Chem., Int. Ed.* **2005**, *44*, 123–126.
20. Li, Z.; Chen, H.; Bao, H. B.; Gao, M. Y. One-Pot Reaction to Synthesize Water-Soluble Magnetite Nanocrystals. *Chem. Mater.* **2004**, *16*, 1391–1393.
21. Li, Z.; Wei, L.; Gao, M. Y.; Lei, H. One-Pot Reaction to Synthesize Biocompatible Magnetite Nanoparticles. *Adv. Mater.* **2005**, *17*, 1001–1005.
22. Hu, F. Q.; Wei, L.; Zhou, Z.; Ran, Y. L.; Li, Z.; Gao, M. Y. Preparation of Biocompatible Magnetite Nanocrystals for *in Vivo* Magnetic Resonance Detection of Cancer. *Adv. Mater.* **2006**, *18*, 2553–2556.
23. Hu, F. Q.; Li, Z.; Tu, C. F.; Gao, M. Y. Preparation of Magnetite Nanocrystals with Surface Reactive Moieties by One-Pot Reaction. *J. Colloid Interface Sci.* **2007**, *311*, 469–474.
24. Liu, S. J.; Jia, B.; Qiao, R. R.; Yang, Z.; Yu, Z. L.; Liu, Z. F.; Liu, K.; Shi, J. Y.; Han, O. Y.; Wang, F.; *et al*. A Novel Type of Dual-Modality Molecular Probe for MR and Nuclear Imaging of Tumor: Preparation, Characterization and *in Vivo* Application. *Mol. Pharmaceutics* **2009**, *6*, 1074–1082.
25. Jia, Q. J.; Zeng, J. F.; Qiao, R. R.; Jing, L. H.; Peng, L.; Gu, F. L.; Gao, M. Y. Gelification: An Effective Measure for Achieving Differently Sized Biocompatible Fe_3O_4 Nanocrystals through a Single Preparation Recipe. *J. Am. Chem. Soc.* **2011**, *133*, 19512–19523.
26. Liu, S. J.; Han, Y. C.; Qiao, R. R.; Zeng, J. F.; Jia, Q. J.; Wang, Y. L.; Gao, M. Y. Investigations on the Interactions between Plasma Proteins and Magnetic Iron Oxide Nanoparticles with Different Surface Modifications. *J. Phys. Chem. C* **2010**, *114*, 21270–21276.
27. Moghimi, S. M.; Hunter, A. C.; Murray, J. C. Long-Circulating and Target-Specific Nanoparticles: Theory to Practice. *Pharmacol. Rev.* **2001**, *53*, 283–318.
28. Brigger, I.; Morizet, J.; Aubert, G.; Chacun, H.; Terrier-Lacombe, M. J.; Couvreur, P.; Vassal, G. Poly(ethylene glycol)-Coated Hexadecylcyanoacrylate Nanospheres Display a Combined Effect for Brain Tumor Targeting. *J. Pharmacol. Exp. Ther.* **2002**, *303*, 928–936.
29. Jun, Y. W.; Huh, Y. M.; Choi, J. S.; Lee, J. H.; Song, H. T.; Kim, S.; Yoon, S.; Kim, K. S.; Shin, J. S.; Suh, J. S.; *et al*. Nanoscale Size Effect of Magnetic Nanocrystals and Their Utilization for Cancer Diagnosis *via* Magnetic Resonance Imaging. *J. Am. Chem. Soc.* **2005**, *127*, 5732–5733.
30. Deli, M. A. Blood-Brain Barrier Models. In *Handbook of Neurochemistry and Molecular Neurobiology Neural Membranes and Transport*; Lajtha, A., Reith, M. E. A., Eds.; Springer: New York, 2007; pp 29−55.
31. Lohmann, C.; Huwel, S.; Galla, H.-J. Predicting Blood-Brain Barrier Permeability of Drugs: Evaluation of Different *in Vitro* Assays. *J. Drug Target* **2002**, *10*, 263–276.
32. Deli, M. A.; Abraham, C. S.; Kataoka, Y.; Niwa, M. Permeability Studies on *in Vitro* Blood-Brain Barrier Models: Physiology, Pathology, and Pharmacology. *Cell. Mol. Neurobiol.* **2005**, *25*, 59–127.
33. Wegener, J.; Abrams, D.; Willenbrink, W.; Galla, H.-J.; Janshoff, A. Automated Multi-Well Device to Measure Transepithelial Electrical Resistances under Physiological Conditions. *Biotechniques* **2004**, *37*, 590–597.
34. Franke, H.; Galla, H.-J.; Beuckmann, C. T. Primary Cultures of Brain Microvessel Endothelial Cells: a Valid and Flexible Model to Study Drug Transport through the Blood-Brain Barrier. *In Vitro. Brain Res. Protoc.* **2000**, *5*, 248–256.
35. Hoheisel, D.; Nitz, T.; Franke, H.; Wegener, J.; Hakvoort, A.; Tilling, T.; Galla, H.-J. Hydrocortisone Reinforces the Blood-Brain Barrier Properties in a Serum Free Cell Culture System. *Biochem. Biophys. Res. Commun.* **1998**, *244*, 312–316.
36. Franke, H.; Galla, H.-J.; Beuckmann, C. T. An Improved Low-Permeability *in Vitro*-Model of the Blood-Brain Barrier: Transport Studies on Retinoids, Sucrose, Haloperidol, Caffeine and Mannitol. *Brain Res.* **1999**, *818*, 65–71.
37. Xu, G.; Yong, K. T.; Roy, I.; Mahajan, S. D.; Ding, H.; Schwartz, S. A.; Prasad, P. N. Bioconjugated Quantum Rods as Targeted Probes for Efficient Transmigration across an *in Vitro* Blood-Brain Barrier. *Bioconjugate Chem.* **2008**, *19*, 1179–1185.
38. von Wedel-Parlow, M.; Schrot, S.; Lemmen, J.; Treeratanapiboon, L.; Wegener, J.; Galla, H.-J. Neutrophils Cross the BBB Primarily on Transcellular Pathways: An *in Vitro* Study. *Brain Res.* **2011**, *1367*, 62–76.
39. Stepp, P.; Thomas, F.; Lockman, P. R.; Chen, H.; Rosengart, A. J. *In Vivo* Interactions of Magnetic Nanoparticles with the Blood-Brain Barrier. *J. Magn. Magn. Mater.* **2009**, *321*, 1591–1593.
40. Rempe, R.; Cramer, S.; Huwel, S.; Galla, H.-J. Transport of Poly(n-butylcyano-acrylate) Nanoparticles across the Blood-Brain Barrier *in Vitro* and Their Influence on Barrier Integrity. *Biochem. Biophys. Res. Commun.* **2011**, *406*, 64–69.
41. Perriere, N.; Demeuse, P. H.; Garcia, E.; Regina, A.; Debray, M.; Andreux, J. P.; Couvreur, P.; Scherrmann, J. M.; Temsamani, J.; Couraud, P. O.; *et al*. Puromycin-Based Purification of Rat Brain Capillary Endothelial Cell Cultures. Effect on the Expression of Blood-Brain Barrier-Specific Properties. *J. Neurochem.* **2005**, *93*, 279–289.